

We are IntechOpen, the world's leading publisher of Open Access books Built by scientists, for scientists

6,900

Open access books available

186,000

International authors and editors

200M

Downloads

Our authors are among the

154

Countries delivered to

TOP 1%

most cited scientists

12.2%

Contributors from top 500 universities



WEB OF SCIENCE™

Selection of our books indexed in the Book Citation Index
in Web of Science™ Core Collection (BKCI)

Interested in publishing with us?
Contact book.department@intechopen.com

Numbers displayed above are based on latest data collected.
For more information visit www.intechopen.com



Low-SAR Miniaturized Handset Antenna Using EBG

Kamel Salah Sultan, Haythem Hussien Abdullah and
Esmat Abdel-Fatah Abdallah

Additional information is available at the end of the chapter

<http://dx.doi.org/10.5772/intechopen.70175>

Abstract

Advances in wireless communications have paved the way for wide usage of mobile phones in modern society, resulting in mounting concerns surrounding its harmful radiation. Energy absorption in human biological tissues can be characterized by specific absorption rate (SAR). This value refers to the actual amount of electromagnetic energy absorbed in the biological tissues, thus a lower value of SAR indicates a lower radiation exposure risk to the human body. So, our challenge is to introduce mobile handset antennas with low SAR and operating at all mobile and wireless applications. In this chapter, novel configurations of single-element antenna are designed, simulated, fabricated, and measured. The antennas operate for most cellular applications: global system for mobile (GSM)-850/900, digital cellular system (DCS)-1800, personal communication service (PCS)-1900, universal mobile telecommunication system (UMTS)-2100, and long-term evolution (LTE) bands. The antennas also support wireless applications. The proposed antennas have a compact size and low SAR at all bands. Also, this chapter presents a comprehensive study on the performance of the antenna in the different environments. Furthermore, the antenna performance is tested in the presence of head and hand in free space and in a car. The simulation and measurement results are in good agreement.

Keywords: specific absorption rate (SAR), multiband antenna, monopole, meander, long-term evolution (LTE), industrial, scientific and medical (ISM), wireless local area network (WLAN), electromagnetic bandgap (EBG), printed antenna

1. Introduction

With the rapid growth of communication technologies and the vast increase of mobile services, developing new low specific absorption rate (SAR) antenna with compact size

becomes of great demand in the international market. Furthermore, the new personal mobile handsets are needed to support multimedia (image with good resolution, clear voice, and data communication) anytime anywhere. This announces that new mobile devices are required to back various technologies and to operate in various bands. So, the long-term evolution (LTE) is presented as new mobile generation to give high performance for communication systems. It has high capacity and large speed of mobile networks [1–6].

Vast research works are introduced to diminish the handset antenna in size and cost and to increase the bands that are provided by the antennas. According to Ang et al. [7], an antenna is introduced to cover four bands (global system for mobile (GSM)-900, digital cellular system (DCS)-1800, personal communication service (PCS)-1900, and industrial, scientific and medical (ISM)-2450) at -6 dB as a reference, and this antenna consists of two-layer folded patches with size of $33 \times 16 \times 8$ mm³. Ciaia et al. [8] replace the ISM 2450 band covered in [7] by the UMTS 2100 band at 6-dB bandwidth, the antenna consists of patch with three extra parasitic elements put on the corner of a ground plane. But, the antenna in Ref. [8] has a double size of the antenna in Ref. [7]. Another two different quad-band antennas are introduced in Refs. [9, 10]. According to Tzortzakakis [9], the proposed antenna consists of a monopole and a helix with half size reduction compared to the antenna in Ref. [7]. According to Ku et al. [10], the proposed antenna consists of a folded dual loop antenna with slight size reduction compared to the antenna in Ref. [7]. According to Tang et al. [11], the proposed compact antenna consists of double inverted L-shape, three-meandered strip and a coplanar strip. The antenna covers five bands (GSM-850, GSM-900, DCS-1800, PCS-1900, and the UMTS-2100) (at -6 dB as reference) with 60% reduction in size referred to the antenna in Ref. [9]. According to Li et al. [12], a folded loop antenna is introduced to cover the hepta band (GSM-850, GSM-900, GSM-1800, GSM-1900, UMTS-2100, GPS, and WLAN at -6 dB bandwidth) with slight size increase compared to the antenna in Ref. [11]. According to Young et al. [13], an octa-band antenna with more compact size of $46 \times 7 \times 11$ mm³ is introduced. The antenna covers the following bands: LTE-700, GSM-850, GSM-900, DCS-1800, PCS-1900, UMTS-2100, LTE-2300, and LTE-2500. The antenna introduced by Young et al. [13] has a compact size in addition to covering eight bands for different mobile applications, yet still several bands need to be covered. In addition, it is complicated in the fabrication process due to its multilayer construction.

The vast development of wireless services needs to consider the interactions between the human body, especially human head, and mobile handset, while the human head absorbs the electromagnetic wave that is radiated by the antenna. Some mobile handset antenna characteristics are alerted for its closeness to the human head because of their radiation pattern, radiation efficiency, bandwidth, and return loss. The mutual effects of human head and the antenna have been introduced by many researches [4–6, 14–16].

There are different methods that were used through the last few decades to reduce the SAR such as using other elements as auxiliary antenna, loading a new material such as ferrite, using the electromagnetic bandgap (EBG) structures to reduce surface wave/artificial magnetic

conductors (AMC) surfaces, and finally using metamaterials [3, 4]. A combination of the main antenna and a director or a reflector was introduced in Ref. [17] to increase the effective radiation efficiency and to reduce the SAR. The distance between the antenna and the auxiliary elements is considered as the main drawback of this method for increasing the size and cost of the antenna. According to Jung and Lee [18], the ferrite sheet was used as a protection wall between the antenna and the human body. The disadvantage of the procedure is the utilization of a costly ferrite material that has unique properties of permittivity and permeability to achieve low SAR [3]. In Refs. [3–6], the EBG and metamaterial techniques are used due to their properties. The EBG technique reduces the SAR values up to 75%.

2. Multiband antennas

2.1. First configuration

Sultan et al. [4] introduce printed multiband antennas to cover the most of mobile bands and wireless application. **Figure 1(a)** shows the planar monopole antenna that is inverted L-shape in size and has an electrical length of a monopole of quarter-wavelength at 2350 MHz. The monopole operating bands are (1700–3000) MHz and (4600–5500) MHz. The dimensions of the monopole antenna are $18 \times 6 \times 1.5 \text{ mm}^3$. The antenna is designed with compact dimensions of $20 \times 33 \times 1.5 \text{ mm}^3$. So, the antenna can be easily integrated in small and sleek mobile device. All the labeled dimensions are tabulated in **Table 1**. **Figure 1(b)** shows the full geometry of the mobile with size of $45 \times 110 \times 1.5 \text{ mm}^3$ in conjunction with a prototype of the antenna. The antenna is fabricated using the FR4 substrate ($\epsilon_r = 4.65$) with 1.5-mm thickness and loss tangent of 0.025 as shown in **Figure 1(c)**.

The antenna is composed of a planar monopole and a planar meander line. The meander line increases the path over which the surface current flows and that eventually results in

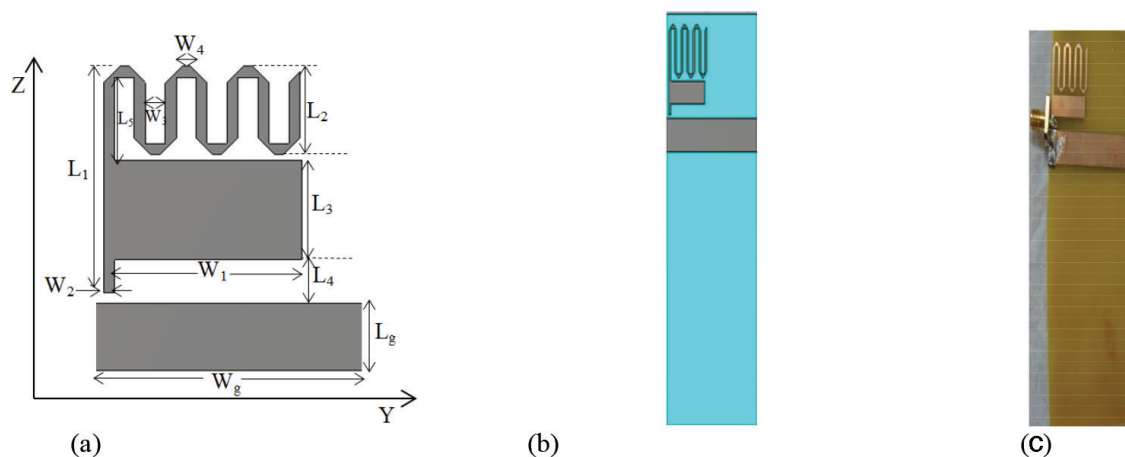


Figure 1. Geometry of the first configuration antenna in mobile phone. (a) Antenna geometry, (b) antenna with full substrate, and (c) antenna prototype.

lowering the resonant frequency. The optimized length of the meander line is 112 mm to operate at 900 MHz. Furthermore, it operates also at the higher frequencies. Where the combination between the monopole and meander line contributes to operate from 1.7 to 7.4 GHz, the distance between the meander line and the monopole is considered as 1 mm that controls the bandwidth matching. Also, the ground plane was chosen to be coplanar with the monopole with size $45 \times 9 \text{ mm}^2$.

The simulated and measured return loss results are introduced in **Figure 2**. One can notice that the simulated and the measured results cover all the proposed mobile and wireless application bands. The antenna operates in the two bands: lower band (0.870–0.970 GHz) and higher band (1.6349–7.4233 GHz) when taking the 6 dB return loss as a reference.

2.2. Second and third configurations

One of the disadvantages of the first configuration antenna is the low front to back ratio and its large SAR value as reported in Ref. [3]. So, if the EBG structure is applied to the antenna, it reduces the surface waves and prevents the undesired radiation from the ground plane as introduced in Ref. [19]. So, the radiation toward the human head is reduced and, hence, the SAR values are also reduced. Although the EBG technique has the advantages of lowering cost and the ease of implementation, the EBG structure still needed more development to produce a practical wideband and small size for multiband applications. Before applying the EBG structure, the antenna dimensions were $30 \times 33 \times 1.5 \text{ mm}^3$. These periodic structures have high electromagnetic surface impedance, which is capable of suppressing the propagation of surface currents and acting as a perfect magnetic conductor in a certain frequency range, so the antenna dimensions are reduced to $20 \times 26 \times 1.5 \text{ mm}^3$. The antenna can be easily integrated in small and sleek mobile device. In this part, two antenna configurations are introduced. In the second configuration, a planar EBG structure is positioned between the user and the handset antenna, while in the third configuration, the EBG structure is positioned in coplanar with the antenna to increase the gain. The planar EBG structure is periodic square patches with dimensions of $9 \times 9 \text{ mm}^2$ and gaps of 1 mm. The whole mobile board of the second configuration and the third configuration is shown in **Figures 3** and **4**. In the second configuration, the EBG is fabricated over the FR4 substrate ($\epsilon_r = 4.5$) with 0.8 mm thickness and loss tangent of 0.025. In the third configuration, the EBG is fabricated in the top layer of the antenna substrate.

Parameter	Value (mm)	Parameter	Value (mm)	Parameter	Value (mm)
L1	24	L5	1	W3	2
L2	14	Lg	9	W4	1
L3	6	W1	17	Wg	45
L4	3	W2	1		

Table 1. Dimensions of first configuration.

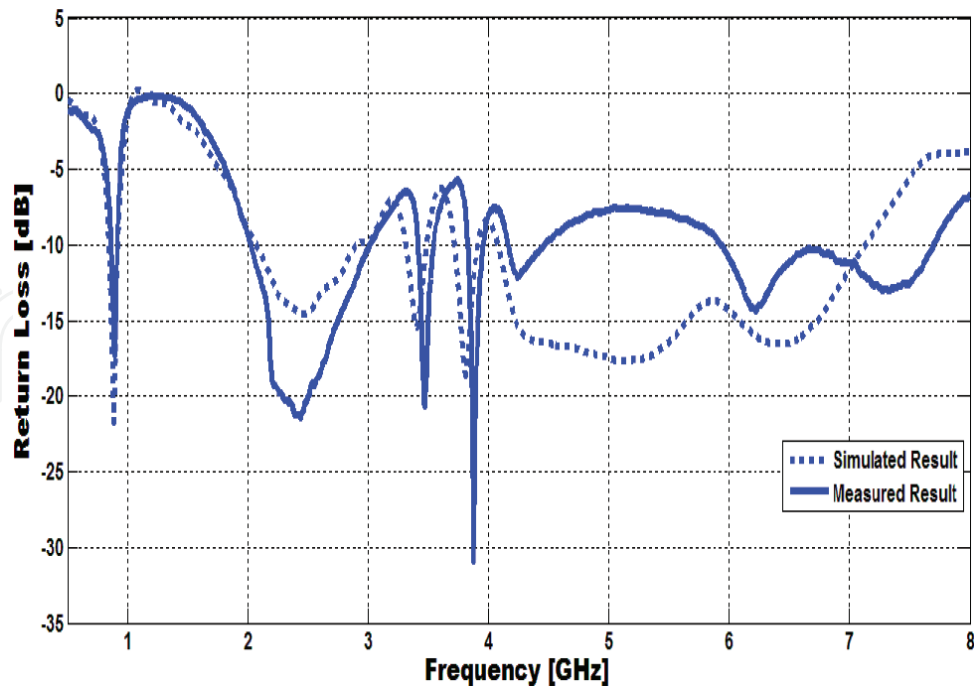


Figure 2. Simulated and measured return loss of the proposed antenna.

The EBG structure is investigated by simulating its behavior within the required band by some iterations. The dimensions of the EBG are selected to be $9 \times 9 \text{ mm}^2$ with a separation of 1 mm to achieve a bandgap in the range from 1.54 to 2.48 GHz. The simulated CST and the experimental results of the return loss of the two antennas are shown in **Figure 5**. The results ensure that the antenna covers all the mobile and wireless applications bands. When taking the 6 dB return loss as a reference, the antenna of the second configuration operates in the two bands (850–1030 MHz) and (1.71–7.8 GHz). The antenna of the third configuration operates in the two bands (830–1000 MHz) and (1.67–8.7 GHz). **Figure 6** shows a comparison between the simulated gain of the antenna with and without EBG structures in the two configurations. From the figure, it is noted that the gain is increased with the use of the EBG structure the antennas dimensions are showed in (**Table 2**).

2.3. Fourth configuration

The first configuration antenna was redesigned before applying the EBG on FR4 material with $\epsilon_r = 4.5$ and $h = 0.8 \text{ mm}$ with compact dimensions of $33 \times 25 \times 0.8 \text{ mm}^3$. The operating bands are 860–1020 MHz and 1.675–8.15 GHz. The EBG structure is embedded on the bottom layer of the substrate as shown in **Figure 7**. The antenna dimensions are showed in **Table 3** for the two cases (with EBG and without EBG). The comparison between the simulated and measured return loss results of the proposed antenna with EBG and without EBG is shown in **Figure 8**. The results reveal that the antenna operates at all the mobile and wireless applications bands. When taking the 6 dB return loss as a reference, the antenna operates in the two bands (from 587 to 977 MHz and from 1.67 to 8.63 GHz). The gain and the radiation efficiency of the fourth antenna are shown in **Table 4**.

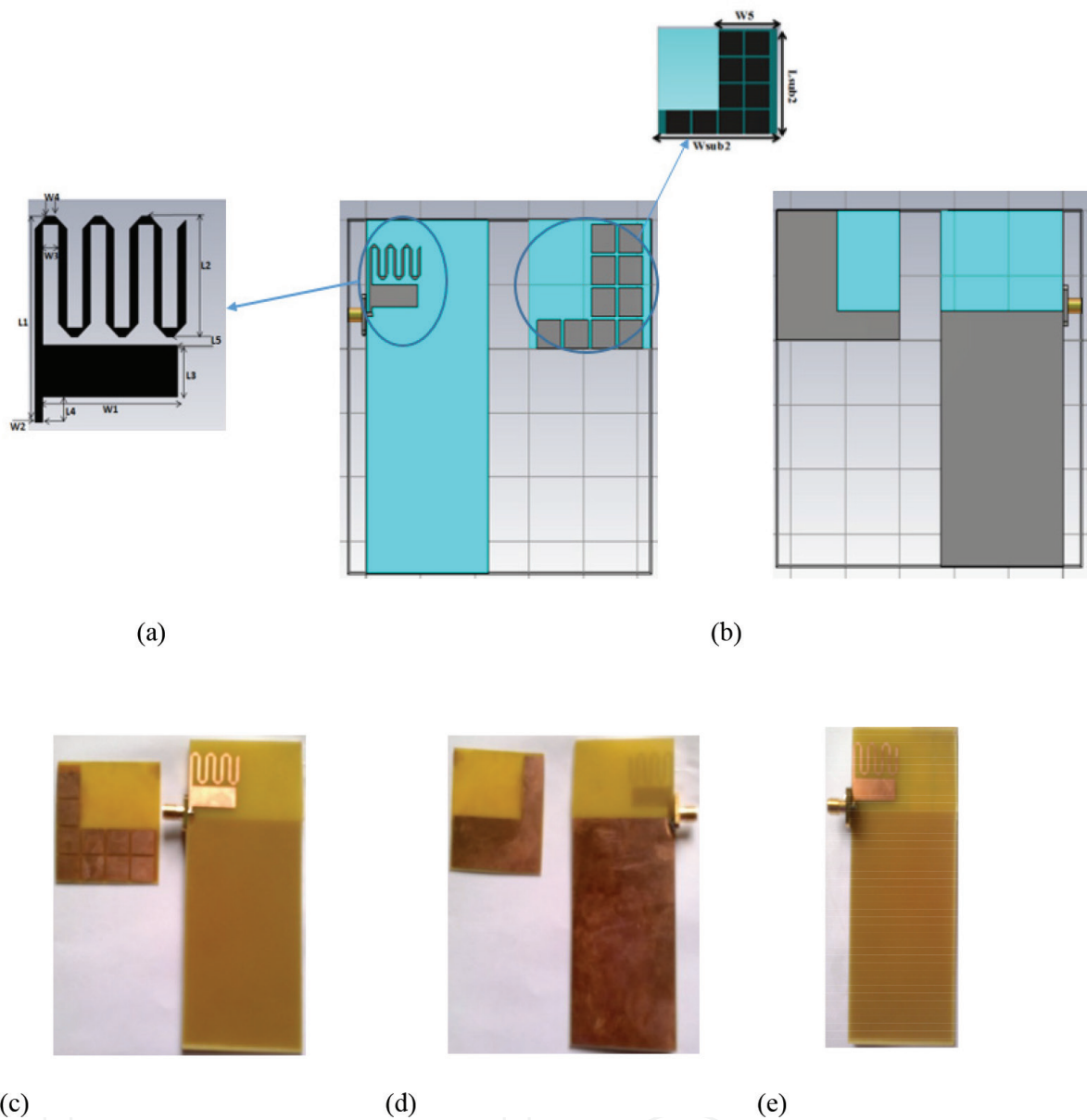


Figure 3. Geometry and prototype of second configuration. (a) Front view of second configuration, (b) back view of second configuration (c) front of the two substrates, (d) back of the two substrates, and (e) second configuration assemble.

When EBG structures interact with electromagnetic waves, they show amazing properties such as frequency pass bands, stop bands, or bandgaps. The characteristics of the EBG structure shown in Ref. [4] ensure that the EBG structures have stop bands at most of the mobile applications and wireless applications bands. This ensures that the EBG structures have high surface impedance (HSI) in these bands, and even when a large electric field along the EBG surface is present, the tangential magnetic field is small. Thus, the generated electric field acts as a magnetic current that radiates in conjunction with the original antenna. The EBG structure is positioned perpendicular to the two antennas: the monopole and the meander line. Without the EBG, the monopole and the meander lines have null radiation at the end-fire directions. With the existence of the EBG, the EBG equivalent magnetic current radiates in the end-fire direction of the two antennas. Thus, some of the radiated energy will be in the

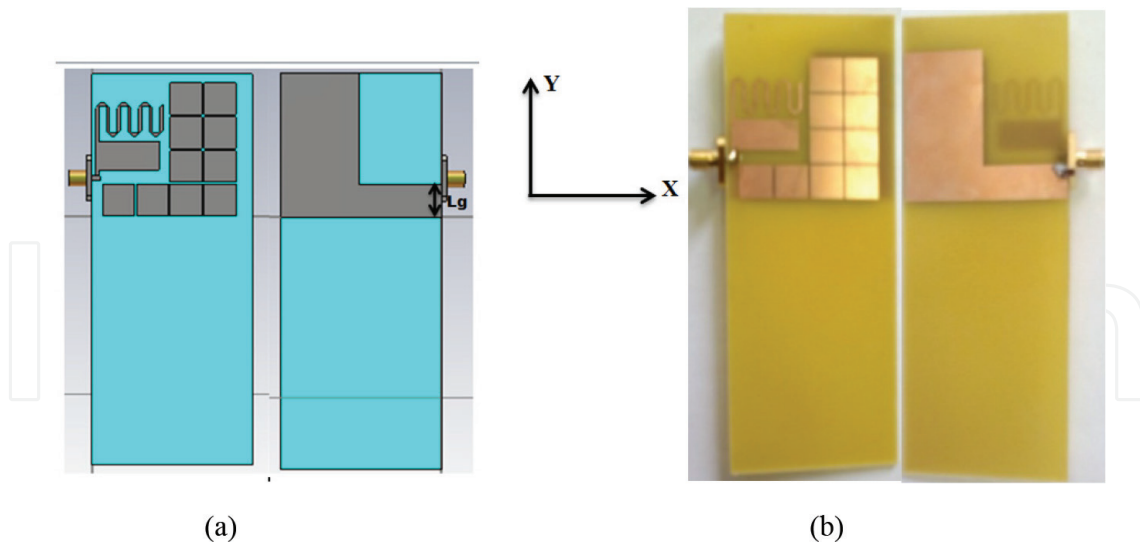


Figure 4. Geometry and prototype of third configuration. (a) Geometry and (b) prototype.

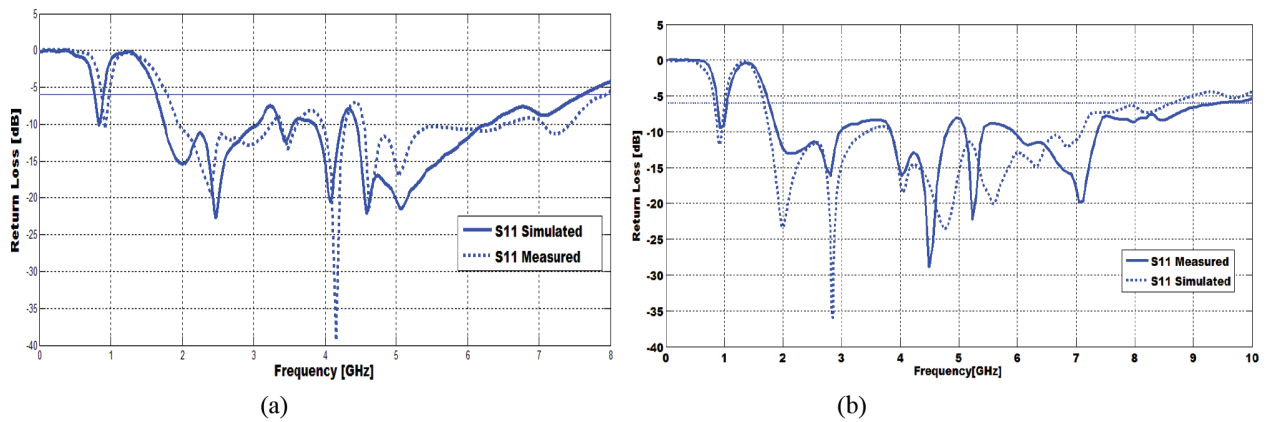


Figure 5. Simulated and measured return loss of the second and third configuration of proposed antenna. (a) second configuration. (b) Third configuration.

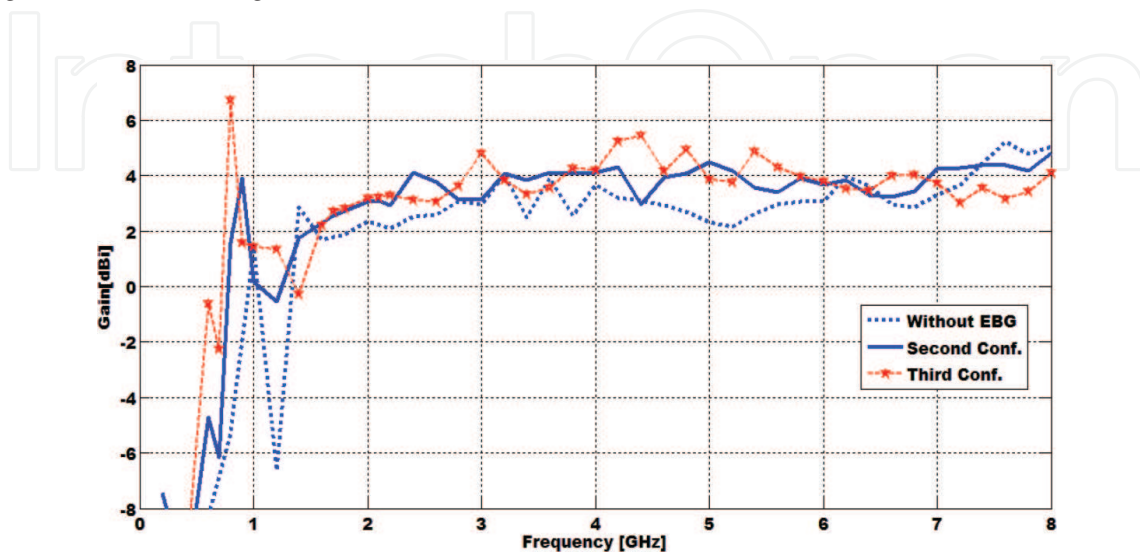


Figure 6. Simulated gain of antennas.

azimuth plane, which reduces the radiation in the elevation direction where the human body exists. Thus, one can conclude that the EBG structure redistributes the radiated energy in such a way that it reduces the radiation toward the human body. **Figure 9** shows the radiation pattern of the proposed antenna in the absence and the presence of the EBG at 1.8 GHz. It is clear that the EBG structures enhance the radiation pattern in the elevation plan. We chose 1.8 GHz

Parameter	Value (mm)	Parameter	Value (mm)	Parameter	Value (mm)
L1	20	L5	1	W3	2
L2	9.5	Lg	79	W4	1
L3	7	W1	17	Wg	45
L4	3	W2	1	Lsub2	40
Wsub2	45	W5	22		

Table 2. Geometric dimensions of the proposed antenna.

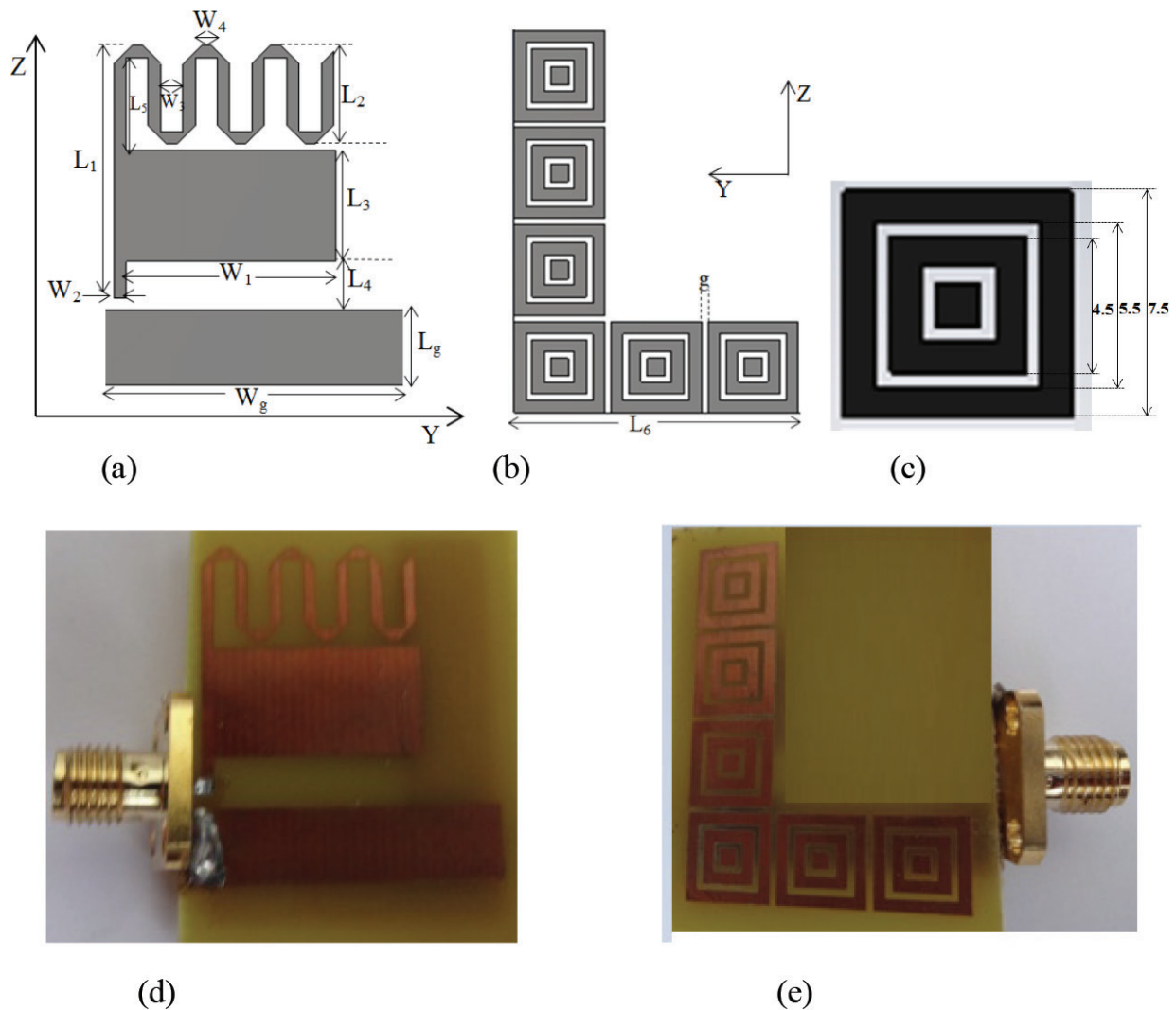


Figure 7. Geometry and prototype of fourth configuration. (a) Front view, (b) back view, (c) unit cell of EBG, (d) front view prototype, and (e) back view prototype.

as an example, but the same enhancement is observed for all the mobile application bands. It appears from **Figure 10** that although the radiation pattern is omnidirectional in the elevation plane, it does not have a null at the end-fire direction of angle 90°. **Figure 10** shows the measured and simulated radiation patterns at frequencies 0.9, 1.8, and 2.1 GHz. Radiation pattern measurements were carried out using SATIMO Anechoic antenna chamber.

Parameter	Without EBG	With EBG	Parameter	With EBG
	Value	Value		Value
$L_1:L_2$	28:14	20.5:8	L_5	7.5
$L_3:L_4$	6:7	9:3	L_6	23.5
$Lg:W_1$	6:17	6:17	G	0.5
$W_2:W_3$	1:2	1:2		
W_4/W_g	1:25	1:25		

Table 3. Antenna dimensions (mm).

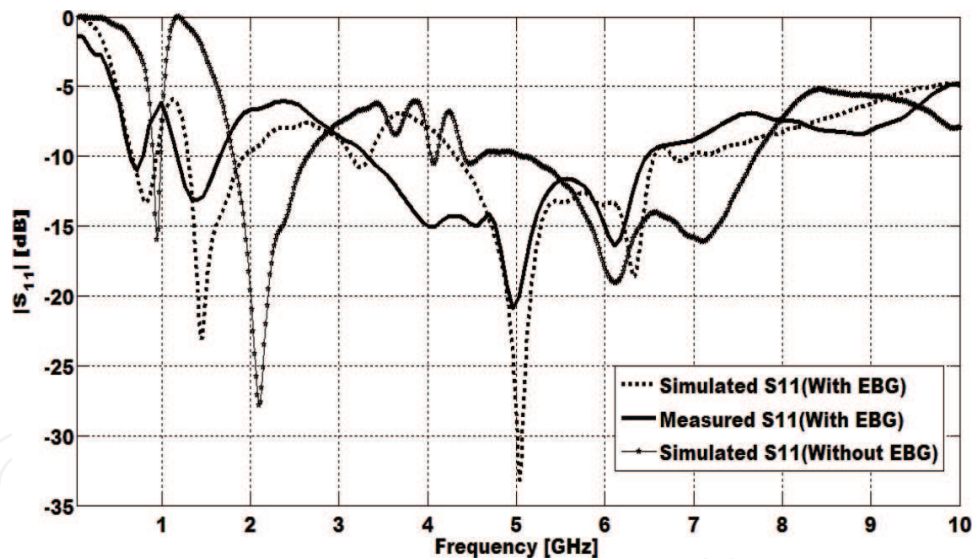


Figure 8. Simulated and measured return loss of the proposed antenna.

F (GHz)		0.9	1.8	2.1
Gain (dBi)	Simulated	2.2	4.4	5.1
	Measured	1.9	4	4.6
Radiation efficiency (%)	Simulated	89	88	81
	Measured	71	68	66

Table 4. Values of gain and radiation efficiency of the proposed antenna.

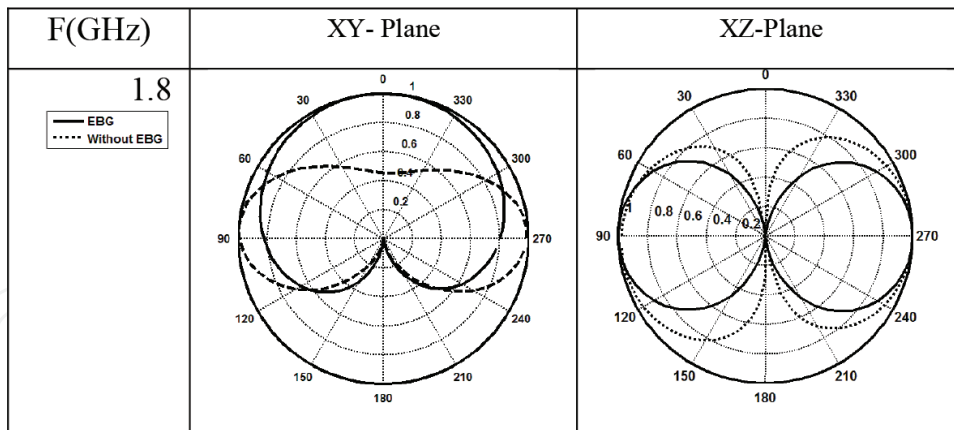


Figure 9. Radiation pattern in the xy and yz planes. The antenna is in the yz plane.

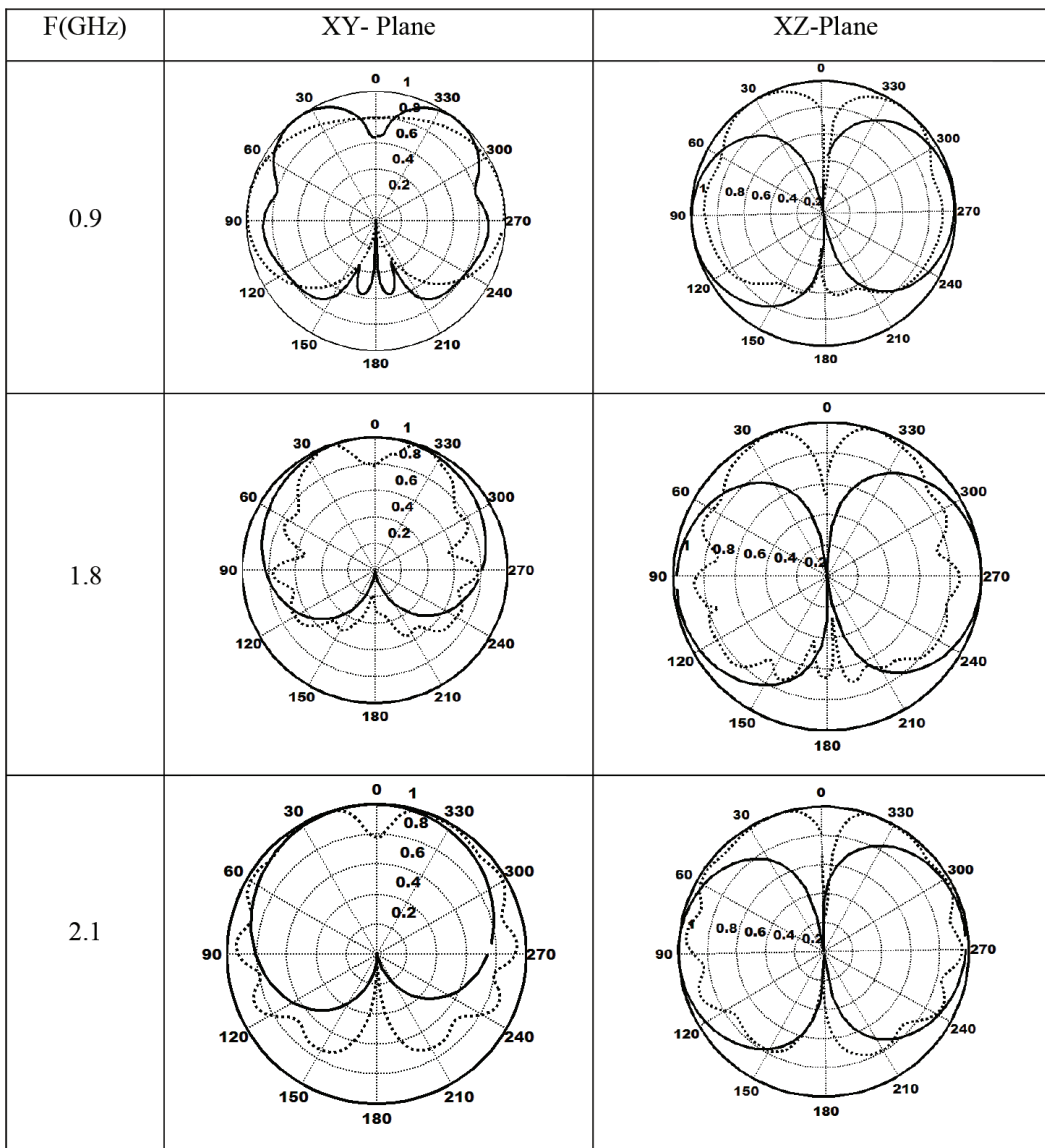


Figure 10. Radiation pattern in the xy and yz planes (a) 0.9 GHz, (b) 1.8 GHz, and (c) 2.1 GHz. The antenna is in the yz plane.

3. SAR calculation

In designing antennas for mobile communications, it is important to investigate the SAR value produced by the radiation from the mobile handsets. The output power of the cellular phone depends on more than one factor such as distance to base station, surrounding environment, frequency band, and technology as shown in Ref. [1]. The reference power of the cellular phone is set to 500 mW at the operating frequencies of 0.9, 1.8, and 2.1 GHz. The SAR values are calculated according to the 10 g standard of the human tissue mass. The SAR calculations are done using the CST Microwave Studio commercial package with Hugo voxel model [20]; the permittivities and the conductivities of the Hugo model tissues are according to the published data in Ref. [21]. The dispersive properties of the tissues are taken into our considerations. As expected, the SAR values depend on many factors such as the operating frequency, the type of antenna, antenna position related to human body, and the relative distance between the human body and the antenna. **Figure 11** shows the SAR calculations on human head model in the presence of the antenna in the ZY plane with and without the EBG structure at 0.7, 0.9, 1.8, and 2.1 GHz. As expected, the SAR values depend on the operating frequency, the antenna types, and the distance between the antenna and the human body. **Table 5** shows the averaged 10 g SAR at the aforementioned operating frequencies when the antenna is close to the body. As the results are scalable when the

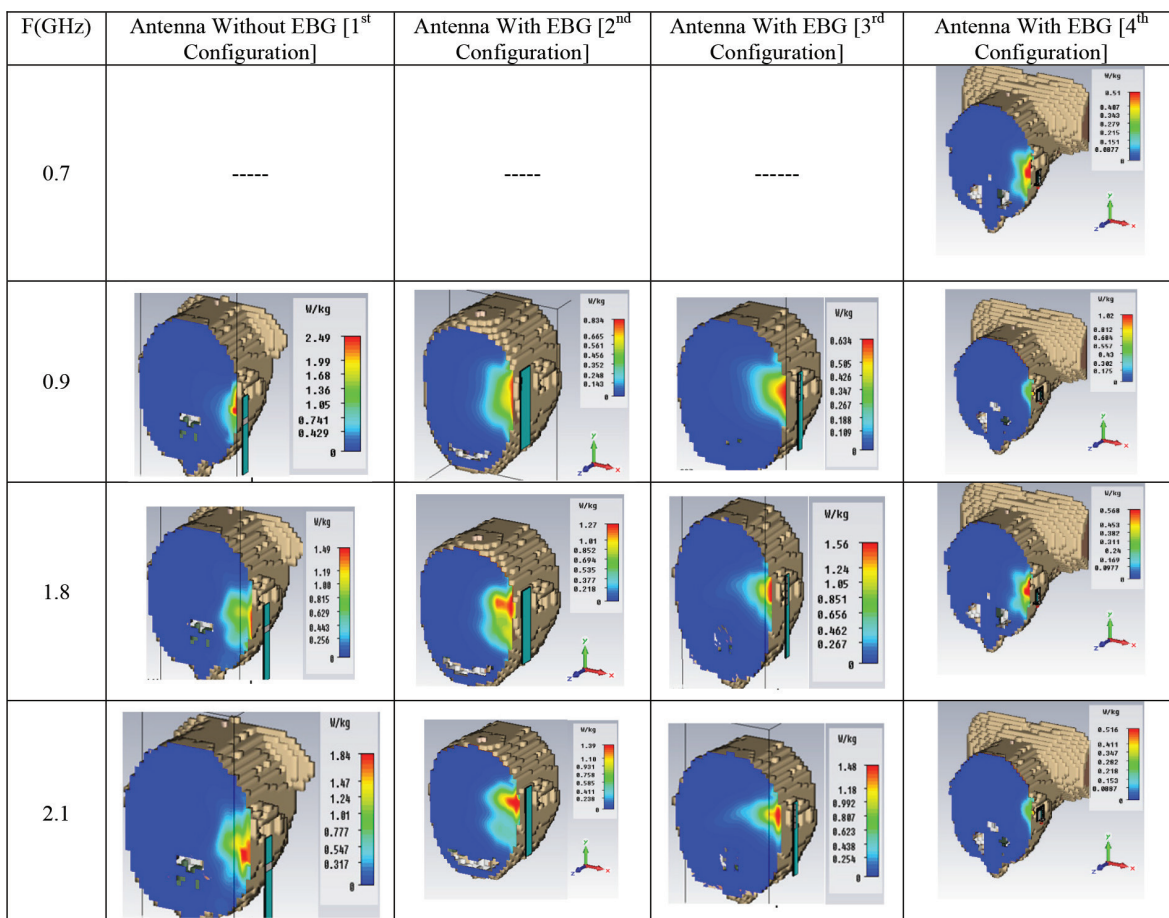


Figure 11. Simulated SAR distribution at 0.9, 1.8, and 2.1 GHz for the three antenna.

power level changes, the SAR values could be controlled by adjusting the separation between the antenna and the head as shown in **Figure 12**, which illustrates that the SAR values decrease with the increase of the separation distance between the antenna and the head. The SAR reduction factor (SRF) and the absorbed power are also tabulated in **Table 5**.

$$\text{SRF} = 100(1 - \text{SAR}_{\text{EBG}}/\text{SAR}_{\text{No EBG}})\% \quad (1)$$

Table 5 ensures that the antenna achieves the IEEE C95.1 and the international commission on non-ionizing radiation protection (ICNIRP) standards [22]. The SAR value is inversely proportional to the distance between the antenna and the head as shown in **Figure 12**. Furthermore, the results are scalable when the power level changes.

Frequency (GHz)	First configuration	Second configuration	Third configuration	Fourth configuration	Absorbed power (rms) W	SRF (%) between (first and fourth)
0.7	–	–	–	0.536	0.0176	–
0.9	2.63 W/kg	0.872 W/kg	0.641 W/kg	1.03	0.03966	60.8
1.8	2.05 W/kg	1.27 W/kg	1.58 W/kg	0.788	0.086	61.5
2.1	1.78 W/kg	1.39 W/kg	1.56 W/kg	0.883	0.0971	50.39

Table 5. Maximum simulated SAR value (antenna closed to the human head).

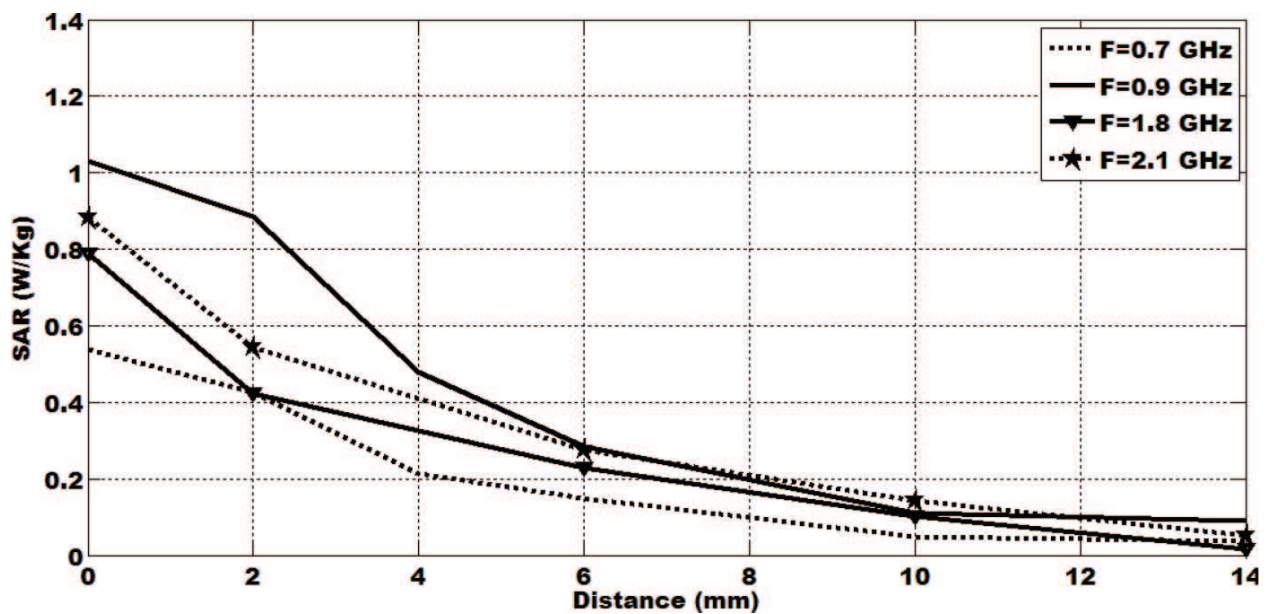


Figure 12. The variation of the SAR value at different frequencies against separation distance between head and antenna for 4th configuration.

4. Antenna in handset

There are several sorts of advanced mobile phones, each exhibiting different qualities and functions. One among these phones may be the “clamshell” alternately foldable portable phone, which has a large LCD, making it really attractive for the end client. It needs two fundamental printed circuit boards (upper and lower PCBs). In practice, the upper printed circuit board (PCB) includes LCD, camera, and speaker. The lower PCB on the other side typically includes radio frequency (RF) circuits and the battery of the phone, and the upper PCB includes keypads and buttons [4]. Another handset of these types is Samsung phone. In this section, we will introduce modeling of both the clamshell and Samsung phones.

4.1. Handset modeling

The advanced mobile phone has various components other than the PCB and the antenna. **Figure 13(a–c)** demonstrate the design of the cell phone without packaging for clamshell-type in the open state or talk state. The two grounds are of a similar size $40 \times 85 \text{ mm}^2$. **Figure 13(d)** demonstrates the perspective of the cell phone in the close state or standby condition. In the open mode, the upper ground is slanted with respect to the focal line of the cell phone with an angle of 15° , which is acceptable inclination for the clamshell cell phone in the talk position. The upper ground is associated with the fundamental ground at a position far from the hinge position or the top edge of the main ground through an extended connecting strip of width 0.5 mm and length 8 mm. While in the close mode, the upper ground is parallel to the primary ground with a separation of 8 mm as appeared in **Figure 13(d)**. The antenna is amassed with the keypad model [20], battery, camera, speaker, RF circuit, and LCD. The installing zone of internal antenna has four choices. **Table 6** demonstrates the favorable position and weakness of every choice. “Impact of hand” implies that holding of client’s hand will cause the move of the operating frequency, and transmitting and receiving become unstable. “Impact of head” defines the moving of operating frequency and raising SAR values. The length of link has an impact on the loss between the antenna and PCB. When a long link is utilized, the signal power will turn out to be low. **Table 6** demonstrates that the best position of the antenna is “Top of Key-Pad side.”

The housing of the mobile is a casing of polyvinyl chloride material polyvinyl chloride (PVC) with permittivity of 2.8 and loss tangent of 0.019, where the total dimensions of the mobile in the closed state are $90 \times 50 \times 14 \text{ mm}^3$ and its wall thickness is 1 mm. **Figure 13(e)** and **(f)** show the mobile after housing with camera and speaker, the camera with 8.5 mm, and it is 6 mm thick. Opposite to the camera is a speaker with the dimensions of 20 mm length and 6 mm width. A large touch screen LCD with size of $70 \times 40 \times 2 \text{ mm}^3$ and a battery with volume $60 \times 35 \times 4 \text{ mm}^3$ are located parallel with a spacing of 1 mm and are connected to the main circuit board via connectors. **Table 7** shows the material properties of the mobile handset parts. **Figure 14** shows Samsung phone with standard dimensions $151.1 \times 80.5 \times 9.4 \text{ mm}^3$ [23], with the same housing material of clamshell mobile, speaker, camera, battery with size $90 \times 60 \times 4 \text{ mm}^3$, RF circuit, and large touch LCD with size $130 \times 70 \times 2 \text{ mm}^3$.

The return loss of the antenna in the two modes of the clamshell mobile (open mode and close mode) is shown in **Figure 15**. There is a slight shift between the results of return loss in the free

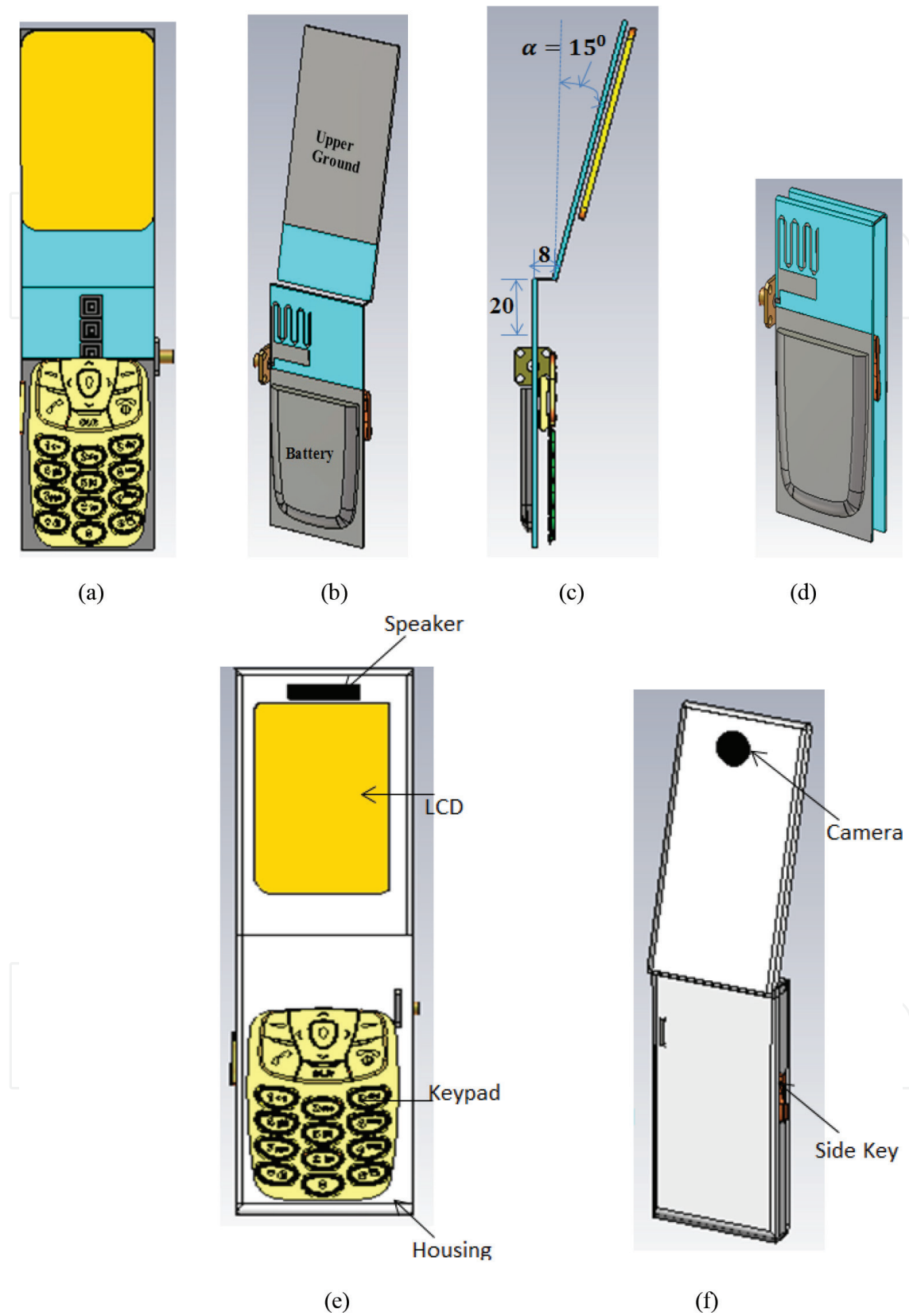


Figure 13. Geometry of the clamshell mobile. (a) Front view of clamshell without packaging. (b) Back view of clamshell without packaging. (c) Side view of clamshell without packaging. (d) Closed mode of clamshell without packaging. (e) Front view of clamshell with packaging. (f) Back view of clamshell with packaging.

Position	Influence for human body	Cable length
Top of LCD	Near the head, large SAR value	90 mm
Bottom of LCD	Little influence of head and hand	40 mm
Top of Key-Pad	Little influence of head and hand	0 mm
Bottom of Key-Pad	Great influence of hand	0 mm

Table 6. Comparison of antenna installing area.

space and in the clamshell handset. In the open case, the effect of the handset components is to mismatch and to shift the operating bands of the antenna, where the bandwidth decreases significantly in the low band. So, the dimensions of internal antenna are designed again to meet the effect of the handset components. The new dimensions of the antenna are $L_2 = 7$ mm, $L_4 = 2.5$ mm, and $W_1 = 18$. In the close case, there is degradation in the impedance bandwidth over the bands. Nevertheless, the operating bandwidth is still better than 6:1 voltage standing wave ratio (VSWR), which is satisfactory to the clamshell phone in the closed case [4].

The requirements and regulations of the mobile handset are developed through the last years by the 3rd generation partnership project (3GPP). The test regulations on various standards were created or are progressing. The Cellular Telecommunications and Internet Association (CTIA)/The Wireless Association is a United States-based global association that serves the interests of the wireless industry by campaigning government organizations and helps with regulation settings. It is vital to test the last antenna execution that impacts the human body [24-32].

The absorption of human body can be characterized as head loss and hand loss when the mobile is in a talking or browsing position. The CTIA organization introduces four different body test cases for any mobile phone (free space test, browsing test, talking test, and talking with hand test) as shown in **Figure 16**. The return loss of those four cases is shown

Mobile parts		Material type	ϵ_r
LCD		LCD film	4.78
Battery		Perfect electric conductor (PEC)	–
RF circuit		PEC	–
Keypad	Digital keys, side key, function keys	Rubber	3.5
	Key lighter	LCD film	4.78
Camera		PEC	–
Speaker		PEC	–
Casing (housing)		PVC	2.8
PCB		FR4	4.5

Table 7. Characteristics of the mobile parts.

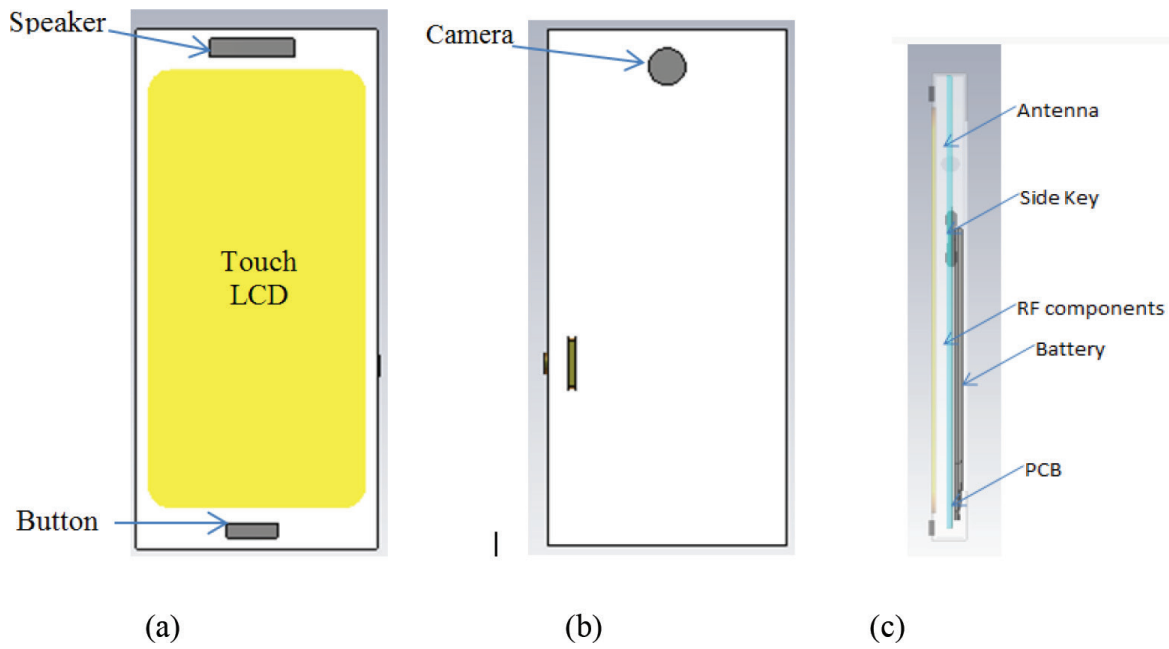


Figure 14. Structure of mobile elements. (a) Front view, (b) back view, and (c) side view.

in Figure 17. The hand and the head have little effect on the antenna impedance matching. Nevertheless, the impedance bandwidth over the operating bands is still acceptable for practical applications of the mobile phone.

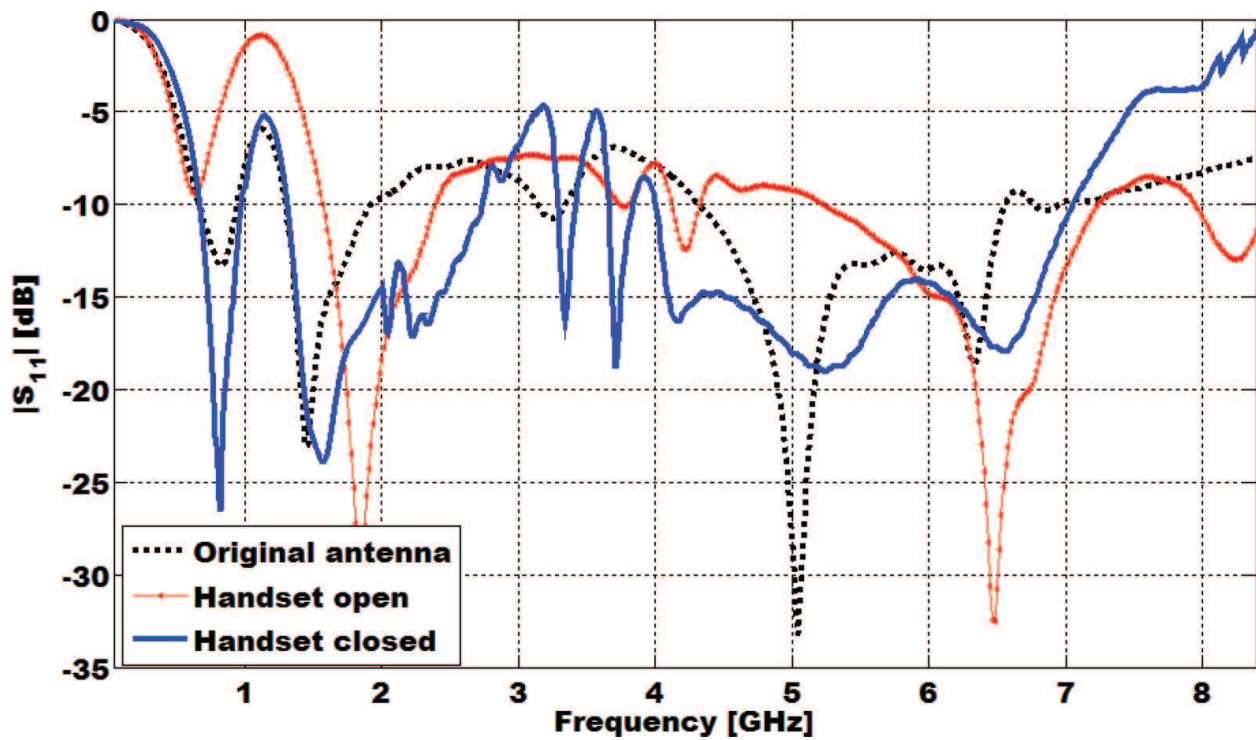


Figure 15. The simulated return loss of original antenna and antenna in handset.

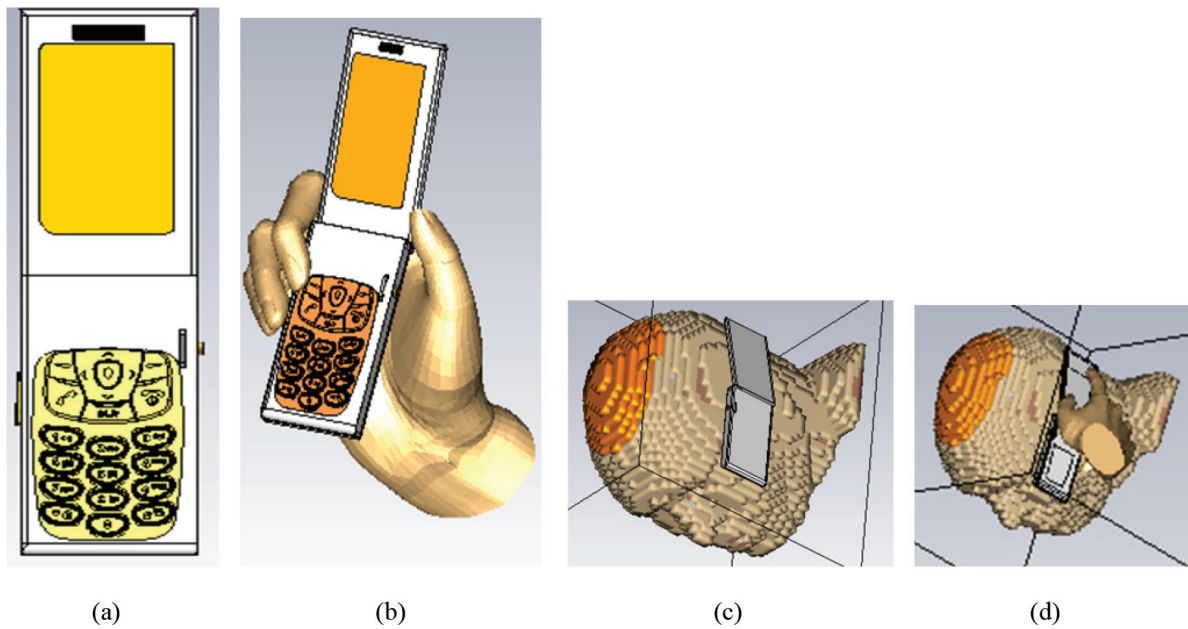


Figure 16. CTIA-defined four different test positions for clamshell mobile: (a) free space, (b) browsing mode, (c) talking position, and (d) talking position with hand.

A Hugo phantom is the specific anthropomorphic mannequin (SAM) phantom, which is defined for SAR measurement. The hand phantoms are defined for talking and browsing modes in evaluating the effects on different phone factors [26].

Table 8 shows the averaged 10 g SAR at the aforementioned operating frequencies for the original antenna and antenna in mobile handset when they are in close proximity to the body. The

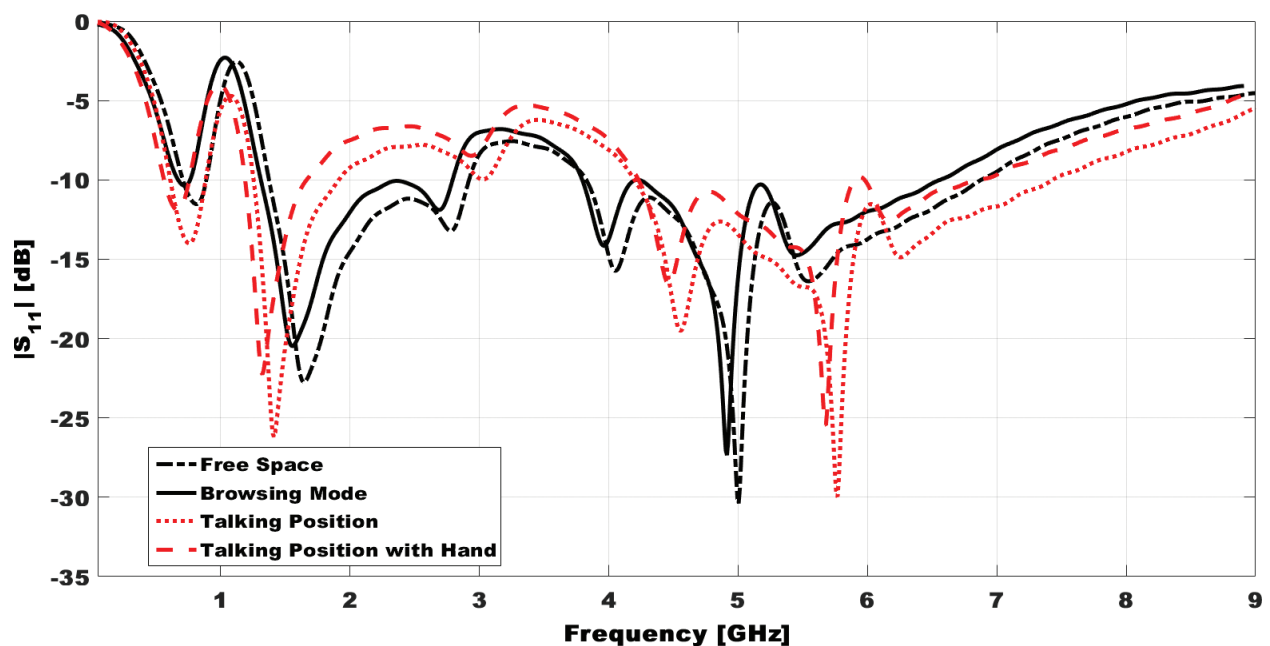


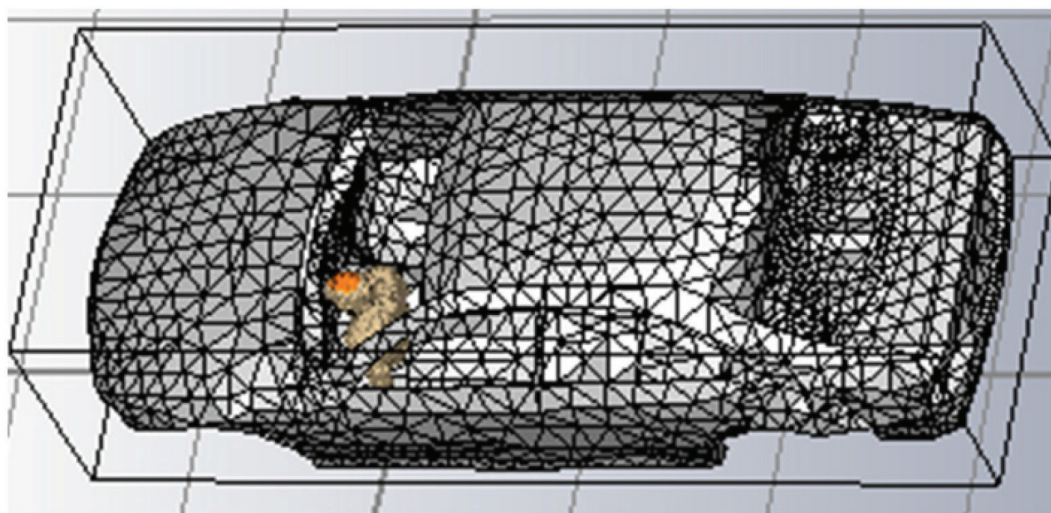
Figure 17. The simulated return loss of antenna in mobile handset in four different test positions.

F (GHz)	SAR (original antenna) W/kg	SAR (antenna in handset) W/kg	SAR (in car) W/kg
0.7	0.536	0.19	0.12
0.9	1.03	0.575	0.47
1.8	0.788	0.48	0.45
2.1	0.883	0.331	0.28

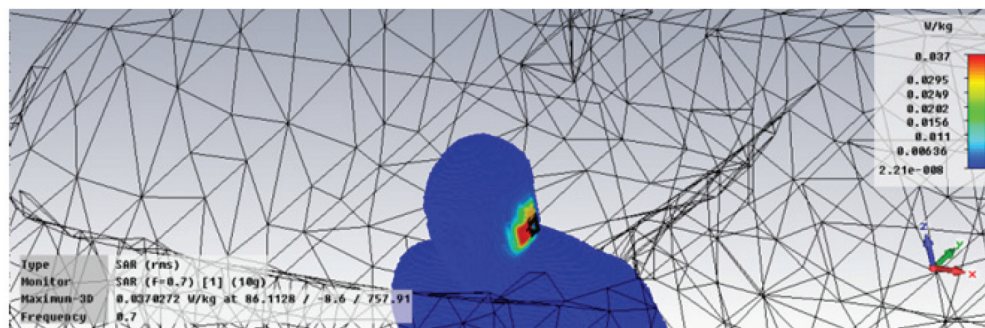
Table 8. Maximum SAR values of the proposed antenna.

F (GHz)	Original antenna (free space)	Handset (free space)	Handset antenna (with human model)
0.7	67%	62%	49%
0.9	65%	60%	61%
1.8	89%	92%	85%
2.1	83%	87%	79%

Table 9. Radiation efficiency.



(a)



(b)

Figure 18. Human model and mobile handset placed within a car model. (a) Human inside car. (b) SAR distribution.

other important concern is the effect of the human body on the antenna performance as shown in **Figure 17**. **Table 9** shows the radiation efficiency of original antenna and antenna in handset in free space and talking position. We locate the human models inside the car, and position it 250 mm from the left and 350 mm from the top of the car model as shown in **Figure 18**. This, in turn, leads us to conclude that the electromagnetic environment of the car has very little effect on the estimated SAR values, and the SAR value is also tabulated in **Table 8**.

5. Conclusion

New four configurations of compact planar antennas that support the mobile applications, ISM band, and wireless services are introduced. The EBG structure is used to minimize the structure size of the antenna, give wide impedance BW, and reduce the SAR values. The SAR values of the all operating frequencies of the antenna are acceptable according to standards in four different modes (free space, talking mode, talking mode with hand, and browsing mode). Furthermore, the SAR values when the human body exists in a car satisfy the standards. Study of the effect of the human body on the antenna performance was also taken into considerations. The antennas have more compact size when compared to other antennas published in literatures. The antennas are simulated using the CST simulator and fabricated using the photolithographic technique. Very good agreement is obtained between the simulated and the experimental results.

Author details

Kamel Salah Sultan^{1,2*}, Haythem Hussien Abdullah^{1,3} and Esmat Abdel-Fatah Abdallah¹

*Address all correspondence to: kamelsultan@eri.sci.eg

1 Electronics Research Institute, El-Tahreer, Giza, Egypt

2 Zewail City of Science and Technology, Giza, Egypt

3 Higher Institution of Engineering and Technology in Damietta new-NDETI, Egypt

References

- [1] Sesia S, Toufik I, Baker M. LTE—The UMTS Long Term Evolution: From Theory to Practice. Chichester, UK: Wiley; 2009
- [2] Johnston S. Review of ongoing research on radio frequencies and health 2002-05. In: Proc. 2nd. Intern. Workshop, Biological Effects of EMFs; Rhodes. 2002. pp. 1004-1013, Oct. 2002
- [3] Villanueva RG, Aguilar HJ, Miranda RL. State of the art methods for low SAR antenna implementation. In: European Conf. on Antennas and Propag. (EuCAP);IEEE, Spain, pp. 1-4, 12-16 April, 2010

- [4] Sultan KS, Abdullah HH, Abdallah EA, Hashish EA. Low SAR, miniaturized printed antenna for mobile, ISM, and WLAN services. *IEEE, Antennas and Wireless Propagation Letters*. 2013;**12**:1106-1109
- [5] Sultan KS, Abdullah HH, Abdallah EA. Comprehensive study of printed antenna with the handset modeling. *Microwave and Optical Technology Letters*. 2016;**58**(4):974-980
- [6] Sultan KS, Abdullah HH, Abdallah EA, Hashish E. Low SAR compact and multiband antenna for mobile and wireless communication. In: 2nd Middle East Conference on Antennas and Propagation, IEEE; Cairo, Egypt, pp. 1-5, 29-31 Dec., 2012
- [7] Ang I, Guo YX, Chia YW. Compact internal quad-band antenna for mobile phones. *Microwave and Optical Technology Letters*. 2003;**38**(3):217-223
- [8] Ciais P, Staraj R, Kossiavas G, Luxey C. Design of an internal quadband antenna for mobile phones. *IEEE Microwave and Wireless Component Letters*. 2004;**14**(4):148-150
- [9] Tzortzakakis M, Langley RJ. Quad-band internal mobile phone antenna. *IEEE Transactions on Antennas Propagation*. 2007;**55**(7):2097-2103
- [10] Ku CH, Liu HW, Lin SY. Folded dual-loop antenna for GSM/DCS/PCS/UMTS mobile handset applications. *IEEE Antennas and Wireless Propagation Letters*. 2010;**9**:998-1001
- [11] Tang CL, Sze JY, Wu YF. A compact coupled-fed penta-band antenna for mobile phone application. In: Proceeding of Asia-Pacific Microwave Conference (APMC); 7-10 Dec. 2010; Yokohama, Japan. IEEE; 2010. pp. 2260-2263
- [12] Li Y, Zhang Z, Zheng J, Feng Z, Iskander MF. A Compact hepta-band loop-inverted F reconfigurable antenna for mobile phone. *IEEE Transactions on Antennas and Propagation*. 2012;**60**(1):389-392
- [13] Young CW, Jung YB, Jung CW. Octaband internal antenna for 4G mobile handset. *IEEE Antennas and Wireless Propagation Letters*. 2011;**10**:817-819
- [14] Sultan KS, Abdullah HH, Abdallah EA, Hashish EA. Low SAR, planar monopole antenna with three branch lines for DVB, mobile, and WLAN. *International Journal of Engineering and Technology IJET*. 2014;**14**(1):70-74
- [15] Sultan KS, Abdullah HH, Abdallah EA. Low SAR, simple printed compact multiband antenna for mobile and wireless communication applications. *International Journal of Antenna and Propagation*, Aug. 2014;**2014**:1-8
- [16] Sultan KS, Abdullah HH. Multiband compact low SAR mobile hand held antenna. *PIER Letter*. 2014;**49**:65-71
- [17] Yew-Siow Tay R, Balzano Q, Kuster N. Dipole configurations with strongly improved radiation efficiency for hand-held transceivers. *IEEE Transactions on Antennas and Propagation*. 1998;**46**(6):798-806
- [18] Jung M, Lee B. SAR reduction for mobile phones based on analysis of EM absorbing material characteristics. *Proceeding of Antennas and Propagation Society International Symposium*; 22-27 June 2003; Columbus, OH, USA. 2003. Vol. 2, pp. 1017-1020

- [19] Sultan KS, Abdullah HH, Abdallah EA, Hashish EA. Low SAR, compact and multiband antenna. In: Progress In Electromagnetics Research Symposium Proceedings, Taipei, Taiwan, pp. 748-751, 25-28 March, 2013
- [20] CST Microwave Studio Suite 2011 User's Manual [Internet]. Available from: www.cst.com
- [21] Gabriel S, Lau RW, Gabriel C. The dielectric properties of biological tissues II Measurements in the frequency range 10 Hz to 20 GHz. *Physics in Medicine & Biology*. 1996;**41**:2251-2269
- [22] IEEE C95.1-2005. IEEE Standards for Safety Levels with Respect to Human Exposure to Radio Frequency Electromagnetic Fields, 3 kHz to 300GHz. New York, NY: Institute of Electrical and Electronics Engineers; 2005
- [23] http://www.gsmarena.com/samsung_galaxy_note_ii_n7100-4854.php
- [24] Zhao K, Zhang S, Ying Z, He S. BSAR study of different MIMO antenna design for LTE application in smart mobile phone. In: Proc. IEEE Antennas Propag. Soc. Conf.; Chicago, IL. 2012
- [25] Ying Z, Liu X. BSAR analysis of different antenna in different size of feature phone. Sony Ericsson Internal Report. 2010
- [26] CTIA Certification Department Program. Test Plan for Mobile Station Over the Air Performance V Method of Measurement for Radiated RF Power and Receiver Performance. [Internet]. Available from: www.ctia.org
- [27] Federal Communications Commission (FCC), BSAR evaluation considerations for handsets with multiple transmitters and antennas, KDB 941255 D01, v01r05.2008
- [28] Liu X, Ying Z. Benchmark of feature mobile phone performance with different antennas including phone size, antenna size and body effects. Sony Ericsson Internal Report. 2010
- [29] CTIA Test Plan for Wireless Device Over-the-Air Performance, Version 3.6.1, Nov. 2016 <https://ctia.org/docs/default-source/certification/ctia-test-plan-for-wireless-device-over-the-air-performance-ver-3-6-1.pdf?sfvrsn=4>
- [30] 3GPP TS 34.114; User Equipment (UE)/Mobile Station (MS) Over-the-Air (OTA) Antenna Performance, V8.4.0, Jun. 2010
- [31] Ying Z. Antennas in cellular phones for mobile communications. *Proceedings of IEEE*, July 2012;**100**(7):2286-2296
- [32] International Non-Ionizing Radiation Association. Guidelines on limits on exposure to radio frequency electromagnetic fields in the frequency range from 100 kHz to 300 GHz. Health Physic Radiation Committee of the International Radiation Protections. 1988;**54**(1):115-123

